

High statistics light meson spectroscopy with the COMPASS spectrometer

S. Paul for the COMPASS collaboration

*Physik Department E18, Technische Universität München
James Franck Str., D-85748 Garching*

Abstract. Hadron spectroscopy is one of the main topics within the COMPASS experiment. Three production mechanisms are used to study exotic states and to search for glueballs: diffractive and central production with pions and protons using a liquid hydrogen target and diffraction and Primakoff reactions with pions impinging on nuclear targets. While the main data taking has been performed in 2008 and 2009, where the statistics of previous experiments has been boosted by a factor 10-100, early measurements with diffractive production on nuclear targets in 2004 have confirmed the existence of an exotic state at a mass around 1.6 GeV. In this paper we report on the final analysis of our 2004 data discussing the evidence for the exotic $\pi(1600)$ and show first insights into the results of the analysis from 2008 data using various final states, thus demonstrating the data quality and potential of the COMPASS data set.

Keywords: exotic mesons, glueball, partial wave analysis, nuclear effects, diffraction, central production

PACS: xxxx

INTRODUCTION

The goal of the COMPASS experiment at CERN[1] is to obtain a better understanding of the structure and dynamics of hadrons, both aspects of non-perturbative Quantum Chromodynamics (QCD). To this end, a rich physics program is conducted covering a wide range of squared momentum transfer Q^2 from a few $10^{-4} \text{ GeV}^2/c^2$ up to $10^2 \text{ GeV}^2/c^2$. In its first phase between 2002 and 2007, COMPASS studied the nucleon spin structure by deep inelastic scattering of $160 \text{ GeV}/c$ muons off a polarized ${}^6\text{LiD}$ or NH_3 target. In a second phase of COMPASS(2008-2009) dedicated experiments with hadron beams of up to $280 \text{ GeV}/c$ were performed. Of particular interest in the field of light meson spectroscopy are states which do not fit into the constituent quark model like glueballs, hybrids, or multi-quark systems. New states have been observed still lacking an unambiguous explanation. In order to gain more insight, experiments with higher statistical accuracy, extending the spectrum to masses beyond $2.2 \text{ GeV}/c^2$, have to be performed.

In addition, Primakoff reactions, i.e. Coulomb scattering of pions or kaons off quasi-real photons from a nuclear target at very small momentum transfers, open the possibility to test effective field theory predictions for fundamental low-energy parameters, such as the polarizabilities of mesons.

THE COMPASS EXPERIMENT

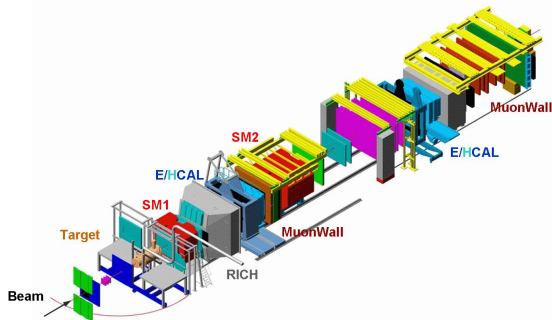


FIGURE 1 : 3D- view of the COMPASS spectrometer. The total length of the apparatus is about 50 m.

The COMPASS physics program mentioned above puts high demands both on the beam and on the experimental setup. The Super Proton Synchrotron (SPS) at CERN delivers proton beams, secondary hadron beams (π , K) and tertiary polarized muon beams with momenta between 100 and $300 \text{ GeV}/c$ at intensities up to $4 \cdot 10^7$ part./s, as required by the small cross sections of the processes under investigation in the two experimental programmes. Figure 1 shows a schematic view of the experimental setup[1]. For the measurements with hadron beams a 40 cm long liquid hydrogen target with a diameter of 35 mm , or simple disks of solid target material are used. The spectrometer has been optimized for large angular acceptance over a broad kinematical range.

The tracks of the incoming beam particle and those of the outgoing particles immediately downstream of the target are measured by several planes of scintillating fibre and Silicon microstrip detectors. In order to maximize the momentum acceptance, the spectrometer is equipped with two dipole magnets (SM1 and SM2 in Fig. 1) with field integrals of 1.0 Tm and 4.4 Tm , respectively, both surrounded by tracking detectors of varying granularity and resolution depending on the distance from the beam axis. Particle identification in the momentum range between 5 and 45 GeV/c is performed by a RICH detector. Electromagnetic and hadronic calorimeters (E/HCAL in Fig. 1) are installed in both stages of the spectrometer. Large acceptance electromagnetic calorimetry with high resolution is of particular importance for decay channels involving π^0 , η or η' .

LIGHT MESON SPECTROSCOPY WITH COMPASS

In the simple $SU(3)_{\text{flavour}}$ constituent quark model light mesons are described as bound states of a quark q and an antiquark \bar{q}' with quark flavors u, d, s . Mesons are characterized by their quantum numbers J^{PC} , with the total angular momentum J , the parity P and the charge conjugation parity C . In the quark model they are given by

$$P = (-1)^{L+1}, \quad C = (-1)^{L+S}, \quad (1)$$

where L is the relative orbital angular momentum of q and \bar{q}' and S the total intrinsic spin of the $q\bar{q}'$ pair, with $S = 0, 1$. In addition to J^{PC} the isospin I and the G parity, defined by

$$G = (-1)^{I+L+S} \quad (2)$$

are conserved quantum numbers in strong interactions.

The quark model model has been quite successful in explaining some of the properties of mesons as well as, to a large extent, the observed meson spectrum, even though it makes no assumptions concerning the nature of the binding force, except that hadrons are postulated to be color singlet states. In QCD, the interaction between colored quarks is described by the exchange of gluons which carry color themselves. Owing to this particular structure of QCD, color-singlet mesons can be composed not only of constituent quarks, but also of other color-neutral configurations like four-quark objects, and excited (constituent) gluons, which then contribute to the quantum numbers of the hadrons: *hybrids* are resonances consisting of a color octet $q\bar{q}'$ pair neutralized in color by an excited gluon, *glueballs* are states composed entirely of excited gluons. Such configurations, however, will mix with ordinary $q\bar{q}'$ states with the same J^{PC} , making it difficult to disentangle the contribution of each configuration. The observation of exotic states with quantum numbers not allowed in the simple quark model, e.g. $J^{PC} = 0^{--}, 0^{+-}, 1^{-+}, \dots$, would give clear evidence for physics beyond the quark model, thus providing a fundamental confirmation of QCD.

The lowest mass glueball has scalar quantum numbers, $J^{PC} = 0^{++}$, and is predicted by LQCD[2] at a mass of $\sim 1.7 GeV/c^2$. The $f_0(1500)$ observed by Crystal Barrel[3] and WA102[4] has been proposed as an experimental candidate for a light glueball, but mixing with ordinary isoscalar $q\bar{q}'$ mesons makes its interpretation difficult. The lowest-lying hybrid, in contrast, is expected[5] to have exotic quantum numbers $J^{PC} = 1^{-+}$, and thus will not mix with ordinary mesons. Its mass is predicted in the region $1.3 - 2.2 eV/c^2$. There are two experimental candidates for a light 1^{-+} hybrid. The $\pi_1(1400)$ was observed by E852[6] and by VES[7] in the reaction $\pi^- N \rightarrow \eta \pi^- N$, and by Crystal Barrel[8, 9] in $\bar{p}n \rightarrow \pi^- \pi^0 \eta$ and $\bar{p}p \rightarrow 2\pi^0 \eta$ Dalitz plot analysis. Another 1^{-+} state, the $\pi_1(1600)$, decaying into $\rho\pi$ [10, 11], $\eta'\pi$ [12, 13], $f_1(1285)\pi$ [14, 15], and $\omega\pi\pi$ [16, 15] was observed in peripheral $\pi^- p$ interactions in E852 and VES. The resonant nature of both states, however, is still heavily disputed in the community[17, 15].

COMPASS is expected to shed new light on these questions, by gathering high-statistics samples for final states containing both neutral and charged particles, using π , K , p as projectiles. Two different production mechanisms are employed: diffractive dissociation and central production, which can be described to proceed via the exchange of one or two Reggeons, respectively, between the beam and the target particle. States with gluonic degrees of freedom are generally believed to be enhanced in reactions in which Pomerons, i. e. Reggeons with vacuum quantum numbers, are exchanged.

Diffractive Dissociation

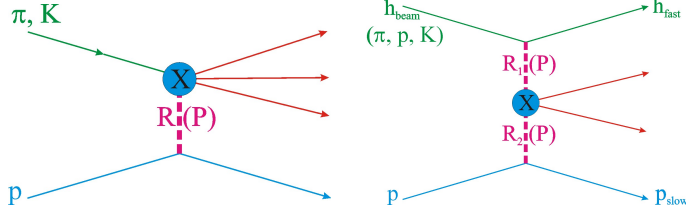


FIGURE 2 : Mechanisms for meson production studied at COMPASS. Left: diffractive dissociation via Reggeon/Pomeron exchange. Right: central production via double Reggeon/Pomeron exchange.

Consider the reaction

$$a + b \longrightarrow c + d, \text{ with } c \longrightarrow 1 + 2 + \dots + n \quad (3)$$

where a is the incoming beam particle, b the target, c the diffractively produced object decaying into n particles, and d the target recoil particle, which stays intact. The reaction proceeds via t -channel exchange of a particle with mass and spin (Reggeon), as indicated in Fig. 2 (left), and is described by 2 kinematical variables: s and $t' = |t| - |t|_{\min}$, where $s = (p_a + p_b)^2$ is the square of the total center of mass energy and $t = (p_a - p_c)^2$ is the square of the four momentum transferred from the in-

coming beam to the outgoing system c . The minimum value of $|t|$ which is allowed by kinematics for a given mass m_c is called $|t|_{\min}$. In the overall center-of-mass frame of the reaction

$$t' = |t| - |t|_{\min} = 2|\vec{p}_a||\vec{p}_c|(1 - \cos \theta_0) \geq 0, \quad |t|_{\min} = 2(E_a E_c - |\vec{p}_a||\vec{p}_c|) - m_a^2 - m_c^2, \quad (4)$$

where E_i , \vec{p}_i and m_i , $i = a, c$ are the energy, 3-momentum and mass of the beam and the diffractively produced system in the center-of-mass system, respectively, and θ_0 is the scattering angle.

The total cross section for diffractive reactions is of the order of 1 – 2 mb. In a fixed target experiment like COMPASS, with a 190 GeV/c π beam impinging on a proton target, even states with masses above 3 GeV/c² can be produced diffractively, although the differential cross section drops as $1/m_c^2$. Their decay products are emitted mostly at small angles with respect to the incoming beam direction, requiring an extremely good angular resolution.

Central Production

Central production of a resonance X proceeds via the fusion of two Reggeons emitted by the beam and the target particle (Fig. 2 right), which both keep their identity. In the center of mass frame both beam and target particles lose only a small fraction x_a and x_b of their energy, respectively. At high beam momenta and for small transverse momentum transfer, the mass of the centrally produced system is $m_X = \sqrt{s x_a x_b}$, where s is the squared center of mass energy. The resonance X carries only a small fraction $x_F \approx 0$ of the maximum longitudinal centre of mass momentum, with

$$x_F \equiv p_L / p_L^{\max} \approx 2p_L / \sqrt{s}, \quad (5)$$

while x_F is close to 1 for the scattered beam particle and close to -1 for the target particle. In a fixed target experiment, the beam hadron appears as the leading particle in the laboratory system (h_{fast}), whereas the target recoil proton is slow (p_{slow}). The centrally produced system can be identified by a gap in rapidity y to the leading beam or target recoil particle, with

$$y = \frac{1}{2} \ln \left(\frac{E + p_L}{E - p_L} \right). \quad (6)$$

With a 190 GeV/c π beam scattered off a proton target, masses up to 1.9 GeV/c² can be produced centrally for $x_a = x_b = 0.1$. Higher mass states require higher energy losses of beam or target particle, and consequently a less clear separation of central production events from different production mechanisms like single diffraction. With $x_a = 0.2$ and $x_b = 0.1$ masses up to 2.7 GeV/c² can be produced, with a rapidity gap to the fast pion of $\Delta y \sim 4.3$ and to the slow proton of $\Delta y \sim 3.3$.

ANALYSIS OF 3π PRODUCTION ON LEAD IN 2004

In order to study the capability of COMPASS to contribute to the field of light meson spectroscopy, diffractive reactions of a $190 \text{ GeV}/c$ π^- beam on a lead target were studied in a short pilot run in 2004 [18]. The $\pi^- \pi^- \pi^+$ final state was chosen because the disputed $\pi_1(1600)$ meson with exotic J^{PC} quantum numbers had previously been reported in this channel. The trigger selected events with one incoming particle and at least two outgoing charged particles detected in the spectrometer. In the offline analysis, a primary vertex inside the target with 3 outgoing charged particles is required. Since the recoil particle was not detected in 2004, a different procedure is applied in order to select exclusive events where the target stayed intact. The beam energy E_a is calculated from the total energy E_c of the 3π system and the scattering angle θ_0 , assuming that the target particle remained intact throughout the scattering process. Then an exclusivity cut is applied, requiring E_a to be within $\pm 4 \text{ GeV}$ of the nominal beam energy. Figure 3 (left) shows the invariant mass of the corresponding events. In our sample of 450000 events, the well-known resonances $a_1(1260)$, $a_2(1320)$, and $\pi_2(1670)$ are clearly visible as bumps in the 3π mass spectrum.

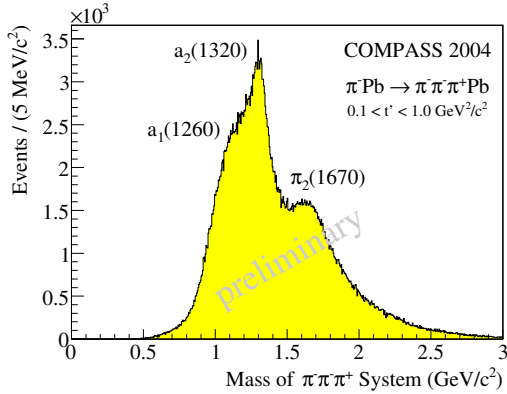


FIGURE 3 : Invariant mass of the 3π system for $0.1 \text{ GeV}^2/c^2 < t' < 1.0 \text{ GeV}^2/c^2$.

A partial wave analysis (PWA) of this data set was performed using a program originally developed at Illinois, but modified at Protvino and Munich. The reaction is assumed to proceed via t -channel Reggeon exchange at high \sqrt{s} , thus justifying the factorization of the total cross section into a resonance and a recoil vertex without final state interaction. Since the exchanged Reggeon carries angular momentum, the incident pion may be excited to a state X with different J^{PC} , limited only by conservation laws for strong interactions. we assume $I=1$ and since $G = -1$ for a system with an odd number of pions, $C = +1$ follows from eq. 2.

The excited state is then assumed to decay into an isobar and an unpaired (bachelor) pion, followed by the decay of the isobar into two pions. In our analysis we consider the isobars $(\pi\pi)_S$ (including the broad $\sigma(600)$ and $f_0(1370)$), $\rho(770)$, $f_0(980)$, $f_2(1270)$, and $\rho_3(1690)$. The spin-parity composition of the excited state X is studied in the Gottfried-Jackson frame, which is the X center of mass frame.

The PWA is done in two steps. In the first step, a mass-independent fit of angular distributions is performed in $40 \text{ MeV}/c^2$ bins of the 3π invariant mass, where a constant production strength for a given wave is assumed:

$$\sigma_{\text{indep}}(\tau) = \sum_{\varepsilon=-1}^1 \sum_{r=1}^{N_r} \left| \sum_i T_{ir}^\varepsilon \psi_i^\varepsilon(\tau) / \sqrt{\int |\psi_i^\varepsilon(\tau')|^2 \tau'} \right|^2 \quad (7)$$

Here, T_{ir}^ε are the production amplitudes and ψ_i^ε the decay amplitudes, the indices i and ε denoting different partial waves, characterized by a set of quantum numbers $J^{PC}M^\varepsilon[\text{isobar}]L$, with J^{PC} as defined above; M the absolute value of the spin projection onto the z -axis; ε the reflectivity, which describes the symmetry under a reflection at the production plane, and corresponds, at high s , to the naturality of the exchanged Regge trajectory; L is the orbital angular momentum between the isobar and the bachelor pion. The ψ_i^ε are constructed based on the isobar model and thus depend on the phase space parameters τ of the 3-body decay, but do not contain any free parameters. Dividing each decay amplitude by its normalization integral compensates its dependence on m inside each mass bin. The sum contains two non-coherent sums over the reflectivity ε and the rank N_r . Assuming that both the target and the recoil particles are nucleons due to the high values of t' considered in this analysis, we set $N_r = 2$, corresponding to helicity-flip and helicity-non-flip amplitudes at the baryon vertex. In addition, the t' dependence of the cross section (especially for $M = 0$ and $M = 1$) is taken into account by multiplying different functions of t' to the decay amplitudes, obtained from the data by making fits in slices of t' . In total 42 partial waves are included in the first step of the fit. It comprises the non-exotic positive reflectivity waves with $J^{PC} = 0^{-+} (M = 0)$, $1^{++}, 2^{-+}, 3^{++}, 4^{-+} (M = 0, 1)$, $2^{++}, 4^{++} (M = 1)$, the exotic $1^{-+} (M = 1)$, and the negative-reflectivity waves $1^{-+}, 2^{++} (M = 0, 1)$, $1^{++}, 2^{-+} (M = 1)$, taking into account all relevant decay modes of the known resonances. It also contains a background wave, characterized by a uniform distribution in the relevant decay angles, which is added incoherently to the other waves. The sets of complex numbers T_{ir}^ε are subject to optimization using an extended maximum likelihood method taking into account the experimental acceptance of the spectrometer, determined from a Monte Carlo simulation of the apparatus. COMPASS has an excellent acceptance for diffractively produced 3π events of the order of 60% over the whole phase space.

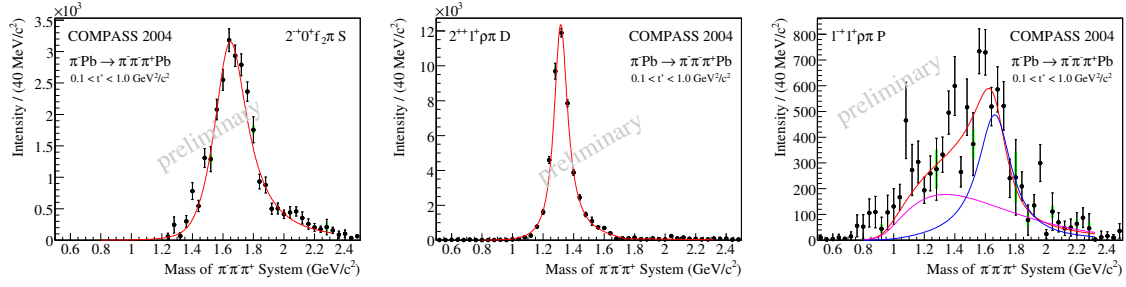


FIGURE 4. Intensities of major waves.

In the second step of the PWA a mass-dependent χ^2 fit to the results of the first step is performed, taking into account the mass-dependence of the produced resonances through relativistic Breit-Wigner functions (and possibly a coherent background). In this fit only a subset of seven waves of the first step is used, the selected waves showing either significant amplitudes or rapid phase motions in the $1.6 \text{ GeV}/c^2$ mass range.

Fig. 4 (top) and (bottom left) show the intensities of the three most prominent waves $1^{++}0^+ \rho\pi S$, $2^{-+}0^+ f_2\pi S$, and $2^{++}1^+ \rho\pi D$. The intensity of the exotic $1^{-+}1^+ \rho\pi P$ wave is shown in Fig. 4 (bottom right, red curve). We observe a broad bump in the intensity for this wave centered at $1.6 \text{ GeV}/c^2$, which we interpret as the $\pi_1(1600)$.

The resonance nature of this wave is demonstrated via its phase differences to the two prominent waves shown in Fig. 4 (top), namely $1^{++}0^+ \rho\pi S$ and $2^{-+}0^+ f_2\pi S$. The latter, shown in Fig. 5 (right), does not exhibit any significant motion between 1.4 and $1.9 \text{ GeV}/c^2$, which is attributed to the fact there are two resonances, $\pi_1(1600)$ and $\pi_2(1670)$, with very similar masses and widths, causing the relative phase motion to vanish. In contrast to this the phase difference to the 1^{++} wave, shown in Fig. 5 (left), clearly shows a rising motion around $1.6 \text{ GeV}/c^2$. As the $a_1(1260)$ is no longer resonating at this mass, this observation can be regarded as an independent verification of the resonating nature of the 1^{-+} wave.

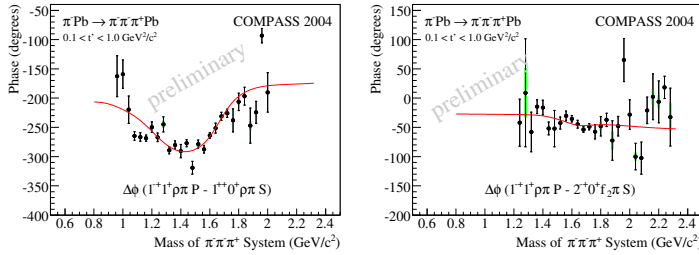


FIGURE 5 : Phase motions of the exotic 1^{-+} wave.

The parameters deduced for the $\pi_1(1600)$ from our fit are a mass of $M = 1.660 \pm 0.010^{+0.000}_{-0.064} \text{ GeV}/c^2$, and a width of $\Gamma = 0.269 \pm 0.021^{+0.042}_{-0.064} \text{ GeV}/c^2$, where the first uncertainty corresponds to the statistical, the second to the systematic error, estimated by testing the stability of the result with respect to various assumptions made in the analysis.

In addition to the Breit-Wigner resonance at $1.6 \text{ GeV}/c^2$, represented by the blue line in Fig. 4 (bottom right), the intensity of the 1^{-+}

wave has a shoulder at lower masses. In our "standard" fit this shoulder is described by a non-resonant background (purple line), possibly caused by a Deck-like effect. In order to study the systematic error and the stability of the $\pi_1(1600)$, we also tried to include a $\pi_1(1400)$ into the fit, but with parameters fixed to PDG values. This did not alter significantly the intensity at $1.6 \text{ GeV}/c^2$ or the phase motions of the 1^{-+} wave.

In contrast to this, the intensity of the $\pi_1(1600)$ resonance is significant: it corresponds to $\sim 16\%$ of the $\pi_2(1670)$ intensity with a significance of 8 sigma. Studies of systematics and fake effects have been performed and are described in ref. [18].

DIFFRACTIVE AND CENTRAL PRODUCTION ON PROTONS

Starting 2008 COMPASS has focussed its activities on hadron scattering using a 40cm long liquid hydrogen target surrounded by a 2 layer recoil detector. This allows to cleanly select exclusive reactions as also coplanarity can be assured in addition to total momentum conservation as mentioned above. This detector is part of the main trigger thus imposing a minimal value of the momentum transfer of $0.07 \text{ GeV}/c^2$. In addition, full electromagnetic calorimetry is available allowing to address also channels with neutral mesons like π^0 and η in the final state. Although not yet optimized in its performance and efficiency results from such final states will be presented throughout this section.

3π analysis from a hydrogen target

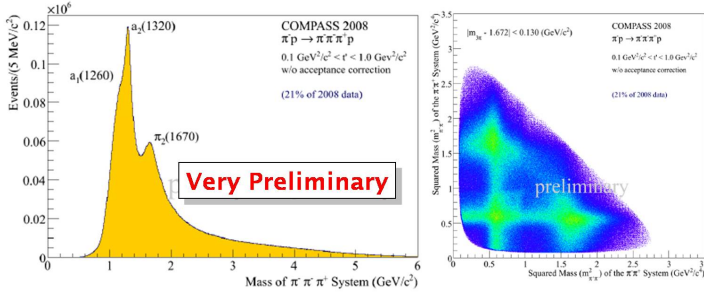


FIGURE 6 : Left: Sample of 3π invariant mass spectrum (t-region selected to match 2004 data). Right: Dalitz plot for events within $\pm 160 \text{ MeV}/c^2$ of the $\pi(1670)$

the two data sets, where high m-values are preferred by nuclear targets (see also [20]).

$\pi^-\pi^0\pi^0$ analysis from a hydrogen target

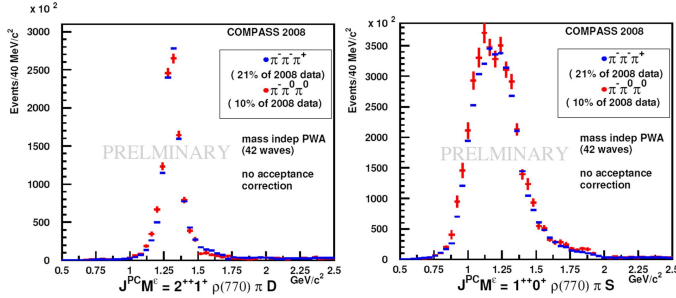


FIGURE 7 : Comparison of isospin partners in the final state ($\rho\pi$). Absolute rates are normalized to a_2 (left) with the a_1 shown on the right. Red dots: neutral modes, blue dots: all charged

The statistics obtained from the two runs in 2008/2009 exceed our previous measurement by about a factor 200. The raw spectrum (about 12% of the whole data set) is shown on the left in fig. 6. The large data set allows to use a finer mass binning of $5 \text{ MeV}/c^2$ (shown) and PWA will be performed in bins of $20 \text{ MeV}/c^2$. The Dalitz plot for the 3π mass region around the $\pi_2(1670)$ is shown on the right of fig.6 in a mass window of $\pm 160 \text{ MeV}/c^2$. Comparing production studied on lead and proton targets a striking difference observed concerns the population of different spin alignments reflected by the different population of $m=0$ and $m=1$ in

An important cross check of all analysis is a test for isospin symmetry in the observed spectra [19]. Comparing final states with two neutral pions to all charged ones different underlying isobars are present and their relative contributions should follow isospin conservation. This is shown in fig. 7 comparing neutral (red) and charged (blue) final states for the two partial waves containing $a_2 \rightarrow \rho\pi$ which is used for relative normalization and $a_1 \rightarrow \rho\pi$, respectively. The analysis takes all isospin factors in the amplitudes into account and shows excellent agreement among the two channels.

$\pi^-p \rightarrow \pi^-\eta(\eta)p$ analysis

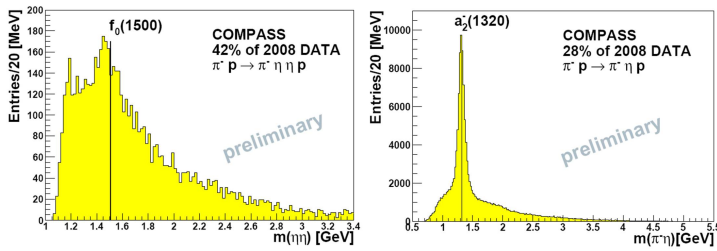


FIGURE 8 : Left: $\eta\eta$ invariant mass in COMPASS with $\eta \rightarrow \gamma\gamma$. Right: Invariant $\pi\eta$ mass from exclusive diffractive production

ing the well known $a_2(1320)$ (about 20% of the COMPASS data set).

In this section we present a first analysis using the η in the final state. η candidates have been selected cleanly from our data samples using the electromagnetic decay of $\eta \rightarrow \gamma\gamma$ only. An exotic state $\pi(1400)$ had been observed in diffractive production by BNL and VES [6, 7] looking into the final state $\pi^-\eta$ and by Crystal Barrel $\pi^-\eta\pi^0$ using $\bar{p}d$ annihilations [8, 9]. However, also this state has been disputed by [17]. Fig. 8 (right) shows the mass spectra for diffractively produced $\eta\pi$ depict-

Central production of $\eta\eta$ has been used successfully to produce the $f_0(1500)$ [22], interpreted as a coherent superposition of different states including the lowest lying glueball. In fig. 8 (left) we show the $\eta\eta$ mass spectrum from COMPASS using $\pi\eta\eta$ final states. A clear sign for the $f_0(1500)$ is observed. The $\pi\eta\eta$ system (not shown) exhibits signals for the $\pi(1800)$ and $\pi_2(1880)$, the $\pi\eta$ subsystem is dominated by the production of $a_0(980)$ and $a_2(1320)$.

5 π final state

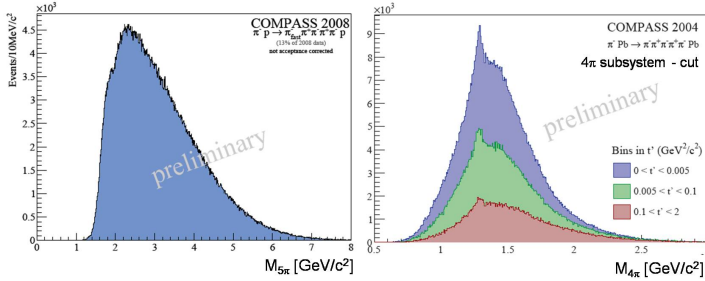


FIGURE 9 : Left: 5π invariant mass. Right: 4π subsystem after some cuts exhibiting the $f_1(1285)$ (example data taken from 2004).

being observed in the 4π subsystem (fig. 9 right - data taken from 2004). The ongoing PWA will include isobars like $f_1, b_1, \eta', \rho(1450)$. The analysis is very complex as a very large waveset has to be considered [20].

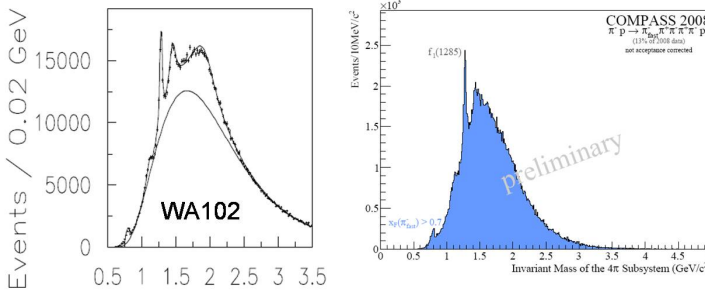


FIGURE 10 : 4π invariant mass in central production. Left: Results from the WA102 experiment [21]. Right: Result from COMPASS based on about 10% of the full statistics. The $f_0(1370)$ is clearly visible together with other resonances (see text)

In order to access high mass states intermediate heavy isobars should be observed. This often leads to large pion multiplicities and the following section addresses analysis with five pions in the final state. Here we distinguish diffractive 5π production and central production using pions where only 4π substates are considered, kinematically separated from the beam and target region. Fig. ?? (left) shows the total 5π spectrum exhibiting the well known $\pi(1800)$. The initial goal is the confirmation of the $\pi_1(1600)$ decaying into $f_1\pi$, the f_1 clearly

being observed in the 4π subsystem (fig. 9 right - data taken from 2004). The ongoing PWA will include isobars like $f_1, b_1, \eta', \rho(1450)$. The analysis is very complex as a very large waveset has to be considered [20].

Centrally produced 4π are kinematically separated from the beam (π_{fast}) and target region (recoil proton). The resulting 4π mass spectra are depicted in fig. 10 are compared to previous measurements of WA102 [21] using pp collisions. WA102 has observed scalar and tensor states like $f_0(1370), f_0(1500), f_0(2000)$ and $f_2(1950)$ [4]. COMPASS in turn has about 100 times more events allowing an extensive PWA also sensitive to small waves in the data set and can compare πp and pp production. The mass spectra are strikingly similar clearly exhibiting a rich structure including the f_1 and other resonances (see also [23]).

Final states with strange mesons

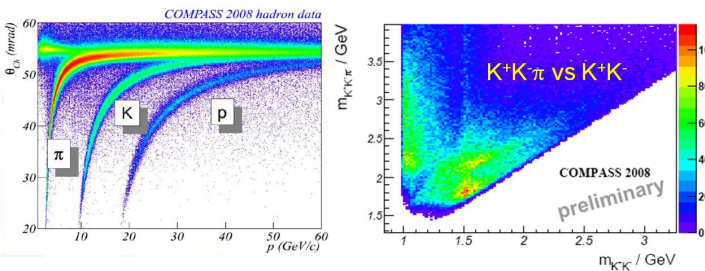


FIGURE 11 : Left: Particle identification in the RICH detector of COMPASS showing the observed Cherenkov angle versus particle momentum. Right: Invariant mass correlations of $K^-K^+\pi$ vs K^-K^+ .

are identified in the RICH (see fig. 11 left) while neutral ones by their well reconstructed decay vertex.

In the following we present a first analysis of events with strange mesons in the final state ([24]). As glueballs should decay with flavor democracy, signals in the non-strange sector must be confirmed in final states with hidden strangeness including KK-pairs. Strangeness in the final states is also often used to search for hybrids owing to partial selectivity in their decay. In addition, kaons combined with pions or kaon pairs lead to rather narrow high mass isobars with low background as can be depicted in the right of fig. 11. Charged kaons

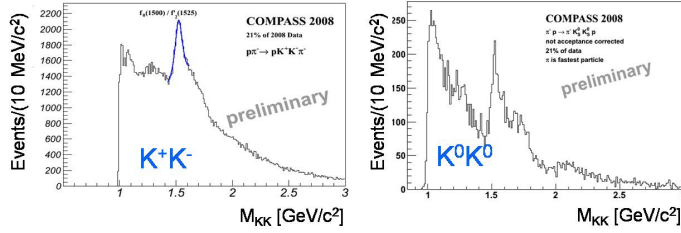


FIGURE 12 : *Left:* Invariant mass of K^-K^+ with $p_{K^-} \leq 30\text{GeV}/c$. *Right:* Invariant mass of $K_S^0K_S^0$.

constraints on the K^- identified in the RICH ($p_{K^-} \leq 30\text{GeV}/c$). The invariant mass spectra of both type kaon pairs are depicted in figure 12 and show a clear structure around the expected $f_0(1500)$.

CONCLUSION

COMPASS with its large acceptance spectrometer has taken data with high intensity pion and proton beams impinging on nuclear and liquid hydrogen targets. Final states including charged and neutral pions, identified kaons and η are being investigated at present with PWA being addressed at present. While a pilot run in 2004 has confirmed the $\pi(1600) \rightarrow \rho\pi$ with similar statistical accuracy as compared to previous experiments the new data sample exceeds the world data by a factor of 10-100, depending on the final state. This will allow to address open issues in the sector of light meson spectroscopy and open the path to study the mass region above $2\text{GeV}/c^2$ with good accuracy.

ACKNOWLEDGMENTS

This work is supported by the the German Bundesministerium für Bildung und Forschung, the Maier-Leibnitz-Labor der LMU und TU München, the DFG cluster of excellence *Origin and Structure of the Universe*.

REFERENCES

1. P. Abbon *et al.*, Nucl. Instr. Meth. A **577**, 455 (2007).
2. Y. Chen *et al.*, Phys. Rev. **D73**, 014516 (2006).
3. C. Amsler *et al.*, Phys. Lett. **B353**, 571 (1995).
4. D. Barberis *et al.*, Phys. Lett. **B474**, 423 (2000).
5. K. J. Juge, J. Kuti, and C. Morningstar, AIP Conf. Proc. **688**, 193 (2004).
6. D. R. Thompson *et al.*, Phys. Rev. Lett. **79**, 1630 (1997).
7. V. Dorofeev *et al.*, AIP Conf. Proc. **619**, 143 (2002).
8. A. Abele *et al.*, Phys. Lett. **B423**, 175 (1998).
9. A. Abele *et al.*, Phys. Lett. **B446**, 349 (1999).
10. G. S. Adams *et al.*, Phys. Rev. Lett. **81**, 5760 (1998).
11. Y. Khokhlov, Nucl. Phys. **A663**, 596 (2000).
12. G. M. Beladidze *et al.*, Phys. Lett. **B313**, 276 (1993).
13. E. I. Ivanov *et al.*, Phys. Rev. Lett. **86**, 3977 (2001).
14. J. Kuhn *et al.*, Phys. Lett. **B595**, 109 (2004).
15. D. V. Amelin *et al.*, Phys. Atom. Nucl. **68**, 359 (2005).
16. M. Lu *et al.*, Phys. Rev. Lett. **94**, 032002 (2005).
17. A. R. Dzierba *et al.*, Phys. Rev. **D73**, 072001 (2006).
18. A. Alekseev *et al.*, COMPASS collaboration, arXiv:0910.5842v1 (2009)
19. F. Nerling, see these proceedings
20. S. Neubert, see these proceedings
21. D. Barberis *et al.*, WA102 collaboration, Phys. Lett. **B413** 217 (1997).
22. D. Barberis *et al.*, WA102 collaboration, Phys. Lett. **B479** 59 (2000).
23. J. Bernhard, see these proceedings
24. T. Schlüter, see these proceedings
25. D. Barberis *et al.*, WA102 collaboration, 9707022v1 9 Jul 1997, Phys. Lett. **B413** 225 (1997).